



3D hydrogeological modeling and visualization of the aquifer system based on borehole data for selecting the optimal well site: a case study in El-Oweinat, Egypt

Ahmed El-Meselhy^{1,2} · Georgy Mitrofanov^{1,3,4} · Alaa Nayef⁵

Received: 2 August 2022 / Accepted: 19 September 2022 / Published online: 25 September 2022
© The Author(s), under exclusive licence to Springer Nature Switzerland AG 2022

Abstract

Visualizing and understanding the aquifer system based on reliable borehole data is increasingly essential in groundwater management and sustainable development. With the possibility of breaking down the wells, decision-makers got extremely concerned about finding the best location for drilling new groundwater wells. Therefore, three-dimensional hydrogeological modeling and visualization of the aquifer system can be used as a decision-aiding tool for selecting the optimum site for drilling new groundwater wells. To build an accurate and reliable 3D model based on geophysical and hydrogeological data, it is essential to develop a workflow methodology that considers the variety of these available borehole data. This method has been developed by a combination of well-logging data (Gamma-ray, SP, and Resistivity) and analyzing step-drawdown pumping tests for 79 groundwater wells, in addition to remote sensing data such as a digital elevation model (DEM) with a high spatial resolution and Landsat images to visualize the surface and subsurface of the study area. Several aquifer properties and characteristics are discussed in this study to help in selecting the optimal well location. Moreover, the 3D hydrogeological model is introduced to visualize the lateral and vertical distribution of the lithostratigraphic layers and to understand the effect of basement rocks on drilling new wells. Three specific suggestions are proposed to enhance the application and efficiency of this 3D modeling and to provide a reference for future applications and developments.

Keywords 3D hydrogeological modeling · Visualization of aquifer system · Groundwater development · Site selection

Introduction

Groundwater is one of the most essential water resources in Egypt. It ranks as the second source of water after the Nile River. Over the last decade, the problem of water resources in Egypt emerged especially after building the Grand Ethiopian Renaissance Dam (GERD) on the Nile River in 2011.

Egypt has been listed among the ten countries threatened by the need for water resources by the year 2025 due to the rapid increase in population (Abdelhaleem and Helal 2015). Therefore, this study aimed to utilize 3D hydrogeological modeling to visualize of the aquifer system and select the optimal well site based on reliable borehole data. This 3D modeling can be used as a decision-aiding tool for selecting the optimum location for drilling new wells in the future.

Many researchers have carried out several previous studies by establishing a three-dimensional geophysical and hydrogeological modeling used for geological applications (Ross et al. 2005; Zhu et al. 2012; Kazakis et al. 2018; Li et al. 2018, 2021; Márquez Molina et al. 2021; Samadi 2022). Moreover, various studies have been conducted on the development of a groundwater visualization system (GVS) to analyze multiple various data sets in areas that need water management and development (Artimo et al. 2003; Robins et al. 2005; Gill 2009; Best and Lewis 2010; Cox et al. 2013; Tian et al. 2016; Qiao et al. 2022). Recently, computer software and hardware developments have enabled

✉ Ahmed El-Meselhy
ahmed.meselhy.geo@gmail.com

¹ Department of Geology and Geophysics, Novosibirsk State University, Novosibirsk, Russia

² Department of Geophysical Sciences, National Research Centre, Cairo, Egypt

³ Institute of Petroleum Geology and Geophysics, Novosibirsk, Russia

⁴ Novosibirsk State Technical University, Novosibirsk, Russia

⁵ National Authority for Remote Sensing and Space Sciences, Cairo, Egypt

the generation of accurate 3D visualization models, and the ability to integrate various digital datasets. As a result, 3D hydrogeological models have become the most effective way to understand and visualize the subsurface aquifer system using different datasets (Oguama et al. 2019; Datta et al. 2020; Fajana 2020; Rane and Jayaraj 2021; Anomohanran et al. 2021; Iserhien-Emekeme et al. 2021; Karami et al. 2022).

Although several studies have been conducted in the study area of El-Oweinat (Nour 1996; Ebraheem et al. 2003), insufficient attention has been paid to building 3D visualization modeling due to the absence of abundant borehole data in previous studies. Therefore, this study contributes to filling out this gap by building up a 3D visualization model using borehole data for 79 groundwater wells in the study area of El-Oweinat, which is located in the southwestern desert of Egypt. Integrating geophysical well-logging data, hydrogeological data, and remote sensing data can help in building this 3D model. In the present study, this 3D hydrogeological model can be used as a decision-making tool for recognizing and finding the optimum site for drilling new groundwater wells depending on reliable borehole data. Moreover, this paper discusses the effect of basement rocks on drilling new groundwater wells and introduce further beneficial information about the extension of the basement rocks, the static water depth (SWD), flow direction, the thicknesses of the aquifer and aquitard layers, aquifer and well loss coefficients, in addition to the well efficiency and total dissolved solids (TDS) in the study area of El-Oweinat.

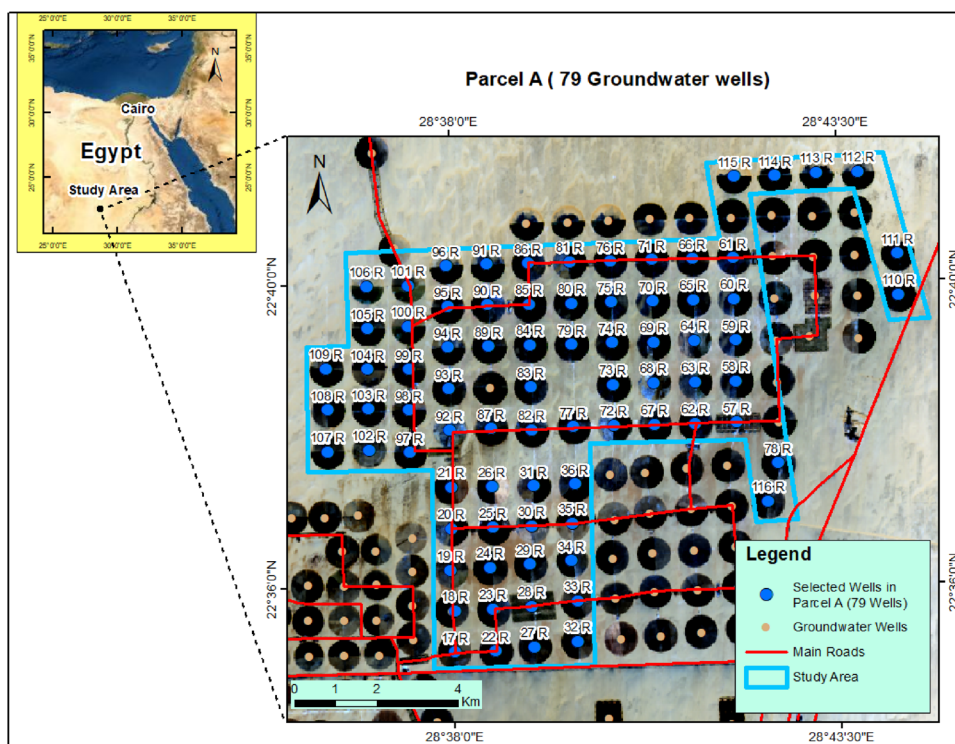
Study area

Regional geology

The study area (Fig. 1) is located in the Southwest of Egypt between latitudes $22^{\circ} 34' 56.49''$ – $22^{\circ} 41' 41.11''$ North, and longitudes $28^{\circ} 35' 56.02''$ – $28^{\circ} 44' 46.85''$ East. The study area covers 84.88 km^2 , where 79 groundwater wells are located in this area (Parcel A). The distance between groundwater wells is 1 km. The depth of the groundwater wells is $\pm 300 \text{ m}$. Groundwater is the only water resource across the arid western desert of Egypt. The Nubian Sandstone Aquifer System (NSAS) is the main exploitable water-bearing formation in the study area (Nour 1996; Ebraheem et al. 2002, 2003; Al-Temamy and Barseem 2010; Masoud et al. 2013; Ibrahim 2019; Araffa and Bedair 2021).

Litho-stratigraphically, the main geological units in the regional study area are described from the oldest to the recent as follows: (a) Precambrian basement, (b) Mesozoic and Lower Tertiary sediments, and (c) Quaternary and Recent deposits (Klitzsch 1979, 1984; Nour 1996; Al-Temamy and Barseem 2010). The Precambrian basement rocks in the regional study area (Fig. 2) are constituted essentially of Aswan-type granites associated with basic igneous and metamorphic rocks. The basement is uncomfortably overlain by a dominating sandy section belonging to the Nubian sandstone. The most remarkable

Fig. 1 Location of the study area



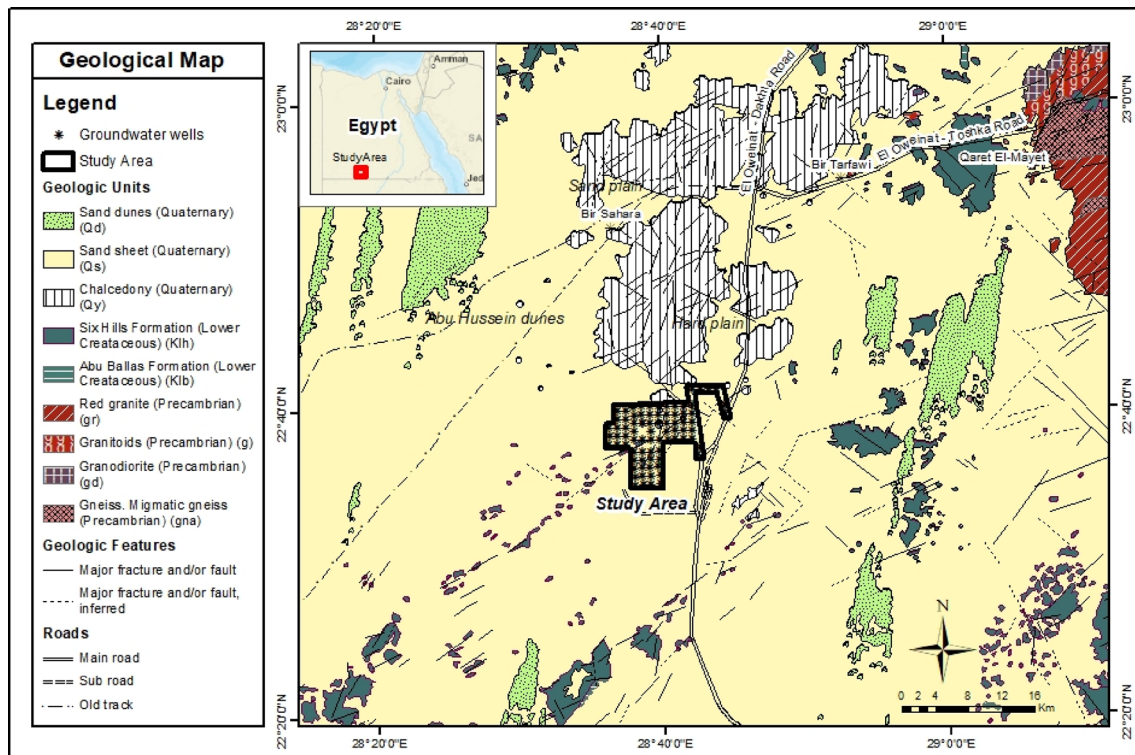


Fig. 2 Geological map for the regional study area (modified after CONOCO 1987)

basement exposure extends from Qaret El-Mayet (Fig. 2) ($23^{\circ} 00' N$ – $29^{\circ} 15' E$), in a northeast direction for more than 40 km. Moreover, other basement features are exposed on the surface at Nusab El-Balgum ($23^{\circ} 20' N$ – $29^{\circ} 15' E$), located 20 km to the north of Qaret El-Mayet, in addition to the basement outcrops which appear at Bir Abu El-Hussein ($22^{\circ} 55' N$ – $30^{\circ} 00' E$) (GPC 1984; Nour 1996). The Mesozoic and lower Tertiary sediments in the regional study area represent the Nubian sequence. The Nubian sandstone sequence is subdivided into different formation units described from the oldest to the youngest as follows: (1) Lower Cretaceous: Six Hills, Gilf Kebir, and Abu Ballas Formations, (2) Upper Cretaceous: Sabaya, Kiseib, and Dakhla Formations, and (3) Lower Tertiary (Paleocene): Kurkur, Garra Formations (CONOCO 1987). The Quaternary and Recent deposits in the regional study area are topping the Nubian Sequence. These sediments are found in considerable extension in the study area. Quaternary deposits are represented as follows: (1) Chalcedony, (2) Playa or lake deposits, and (3) Eolian deposits, which are divided into two main types (Sand dunes) and (Sand sheets). Chalcedony (Fig. 2) occurs around Bir Sahara and overlies the Six Hill formation (GPC 1984; Nour 1996).

The hydrogeological framework in the study area consists of a water-bearing unit known as the Six Hills Formation, which is built up of fine to medium-grained sand and

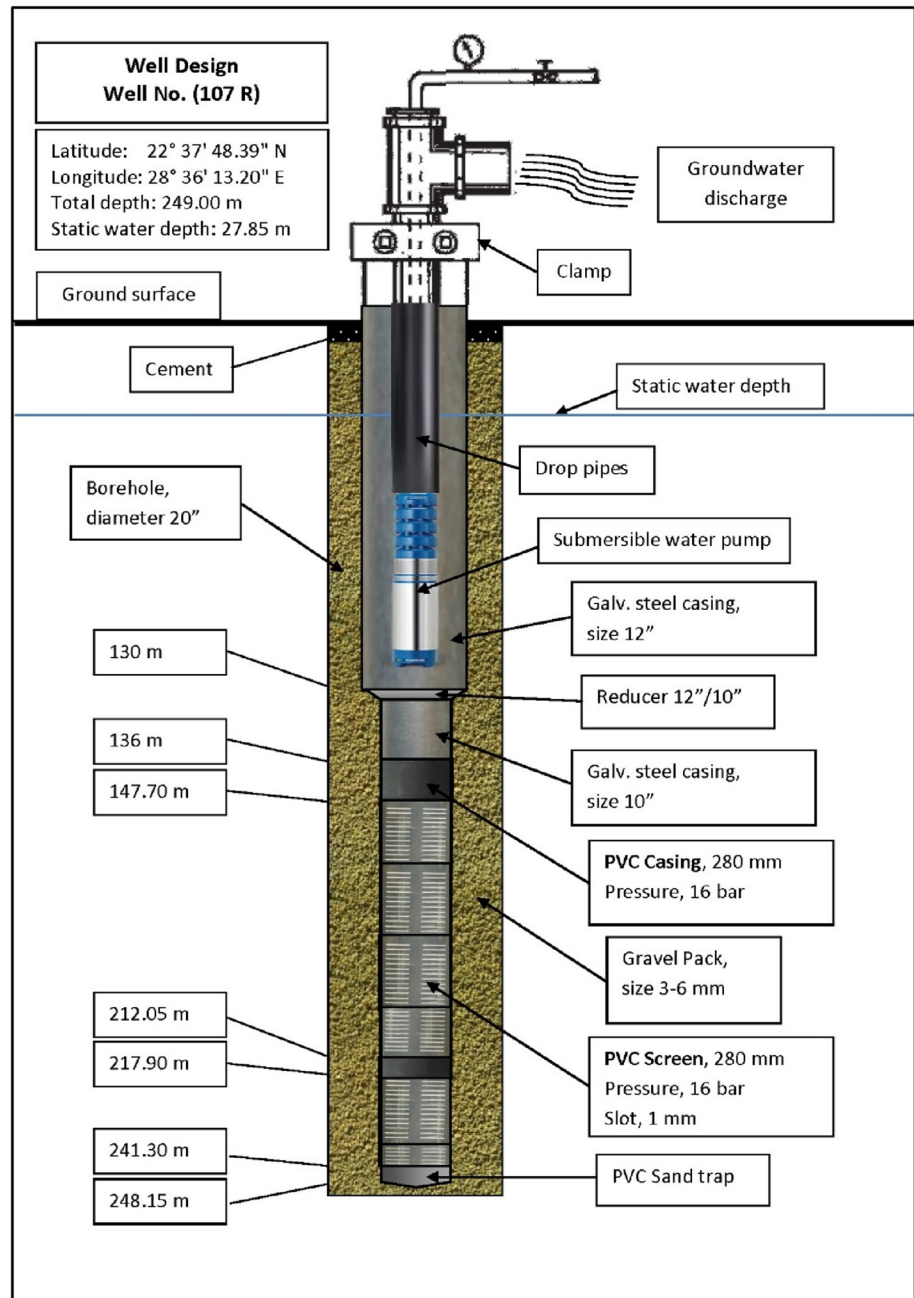
sandstone intercalated by confining beds of shale, clay, and silt. These semi-permeable sediments are discontinuous due to rapid lateral changes of facies (Ebraheem et al. 2002; Al-Temamy and Barseem 2010; Masoud et al. 2013).

Problem identification and objectives

In the study area, groundwater wells are breaking soon after construction, leaving the decision-makers with no option but to drill new wells. Several fundamental reasons can cause water wells to fail early: (1) improper well design and construction, (2) the placement and quality of the materials, (3) incomplete well development, (4) incrustation build-up, (5) corrosion, (6) aquifer problems and (7) over-pumping. The first three causes are related to the expertise and performance of the groundwater well contractor. Incrustation build-up, corrosion, and aquifer problems are related to the characteristics of the aquifer. The last cause, over-pumping, is caused by users of groundwater wells. The cost of constructing a borehole is high, so the issue of selecting the optimum location for drilling new wells should be taken seriously to ensure that these problems do not occur again.

Drilling groundwater wells in the study area (Fig. 3) undergoes several steps or stages which can be summarized as follows: (1) preliminary drilling stage, (2) enlargement of the diameter of the well, (3) casing and screen installation,

Fig. 3 Well design of the groundwater well (107 R) in the study area



(4) gravel pack stage, (5) air development stage, (6) pump development stage and (7) performing pumping tests. After the first stage, sometimes basement rocks are encountered at the bottom of the well. Therefore, instead of wasting money after reaching this depth, the decision maker continues to use this well location.

The main objective of the present study is to select the optimal well location for drilling new groundwater wells by building 3D modeling and visualization of aquifer systems based on borehole data (well-logging, lithological and hydrogeological data), which are integrated with various datasets such as scanned or digitized maps and

satellite imagery to be used as a tool for decision-making. There has been increasing improvement and use of powerful 3D modeling packages such as Petrel (Schlumberger Limited). The user can develop cross sections in different directions within the software to produce 2D and 3D maps and to improve the 3D visibility of the aquifer properties.

The present study will delineate the extension of the basement rocks in the study area. Therefore, this will help the decision-makers to avoid drilling new wells near these locations if the existing wells fail or break down for any reason in the future.

Materials and methodology

The workflow methodology (Fig. 4) adopted in this work can be divided into three categories: (1) Source data, (2) GIS and Geodatabase and (3) Geomodeling.

Regarding source data, borehole data are one of the major data sources for 3D hydrogeological modeling. In the present study, 79 groundwater wells were used for building up the 3D modeling and visualization of the aquifer system based on geophysical well-logging data (Gamma-ray, SP, and resistivity logs) and hydrogeological data (pumping tests), especially the step-drawdown tests, in addition to remote sensing data such as satellite imagery and digital elevation model (DEM).

To establish a geodatabase, the study area’s geological map was scanned, imported into ArcGIS 10.8, and georeferenced to the UTM/WGS84 projection system, zone 35 north. Landsat images and Digital Elevation Model (ALOS PALSAR—Radiometric Terrain Correction RTC) with a

spatial resolution of 12.5 m have been integrated into a multilayer GIS environment. By analyzing the pumping tests for 79 groundwater wells, hydrogeological data and aquifer properties have been determined and stored in GIS database.

Finally, for geomodeling, all of these surface and sub-surface borehole data have been provided as basic data for constructing a three-dimensional hydrogeological model. Hence, all data are imported into Petrel software to build the 3D model. Re-interpretation and correlation between well-logging data have been carried out using Petrel software to determine the lithofacies in the study area based on the description of the cutting samples and re-interpretation of well-logging data. Consequently, different cross sections within the software were developed and produced to build the 3D model.

Therefore, to build the 3D hydrogeological model, the following steps have been followed:

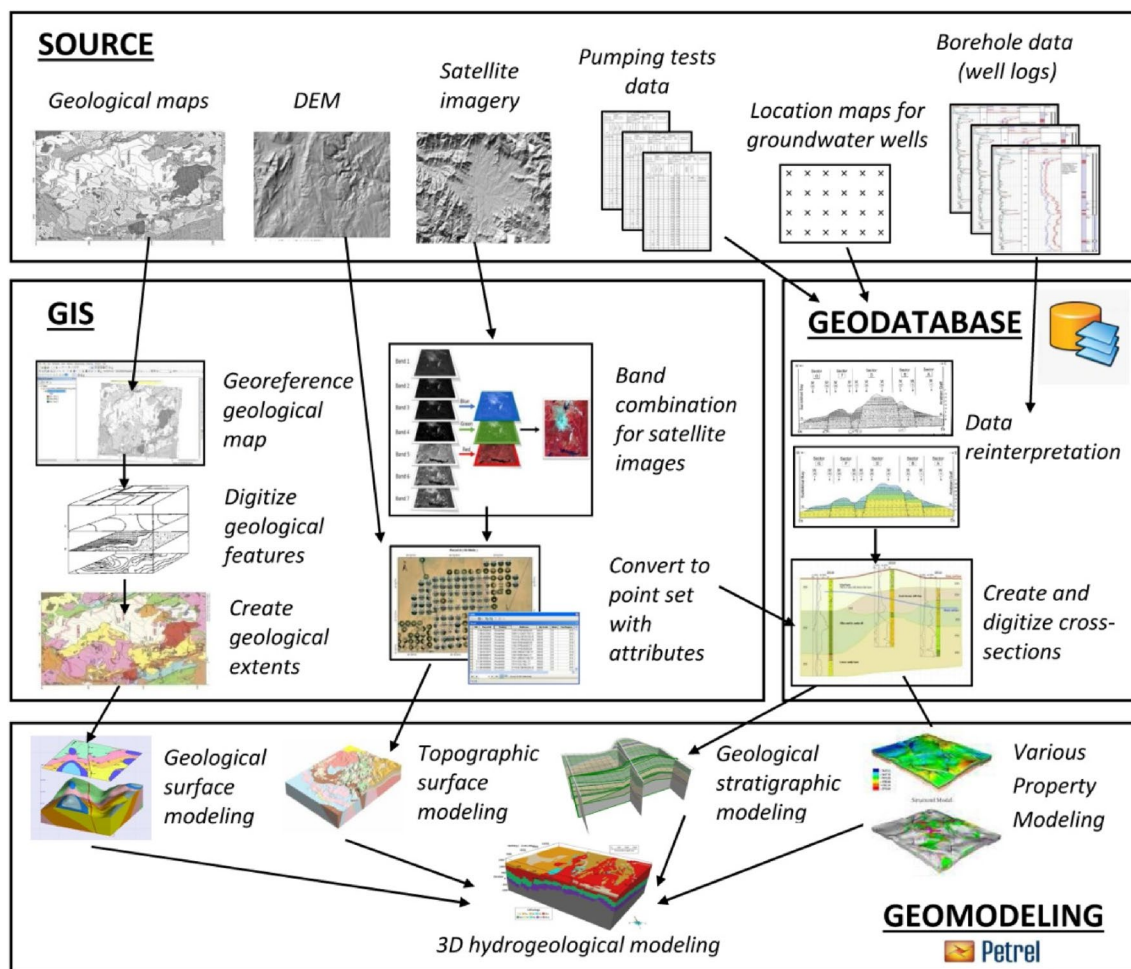


Fig. 4 The workflow methodology used to build the 3D Model in the study area

1. Digitizing the well-logging data with quality control (QC) for 79 groundwater wells and analyzing pumping tests.
2. Importing well-logging data and hydrogeological data into Petrel software.
3. Re-interpretation of well logs and determining the thicknesses of the sandstone, shale, and basement layers based on reliable data of both well logs and the description of the lithology from cutting samples.
4. Correlation between well-logging data and creating 2D cross sections in different directions (i.e., East–West and North–south)
5. Creating spatial maps for different parameters to depict the properties and characteristics of the aquifer system in 3D views.
6. Building up a 3D hydrogeological model based on the borehole data for 79 groundwater wells in the parcel (A) using Petrel software for visualization of the aquifer system.

This 3D hydrogeological model can be used for the management and sustainable development of groundwater resources and for helping the decision-makers in selecting the optimal location for drilling new wells in the future.

Results and discussion

Topography and digital elevation model (DEM)

Topography is an important factor in selecting the optimal location for drilling groundwater wells. The flat areas and sand sheets are considered the optimal places to drill new wells. In contrast, the areas near sand dunes are generally the worst locations due to the effect of these dunes on agricultural activities and the center pivot irrigation system.

DEM with a spatial resolution of 12.5 m (Fig. 5) indicates that the study area is a flat area and the mean elevation value is 270 m above mean sea level. The slope, hillshade and aspect maps have been extracted from DEM to show the ground relief in the study area.

The hillshade map (Fig. 5) is a very useful and powerful thematic map for visualization of surface relief in the study area. The hillshade map reveals that the area under investigation is a nearly flat area which is a perfect environment for agricultural activities and drilling groundwater wells.

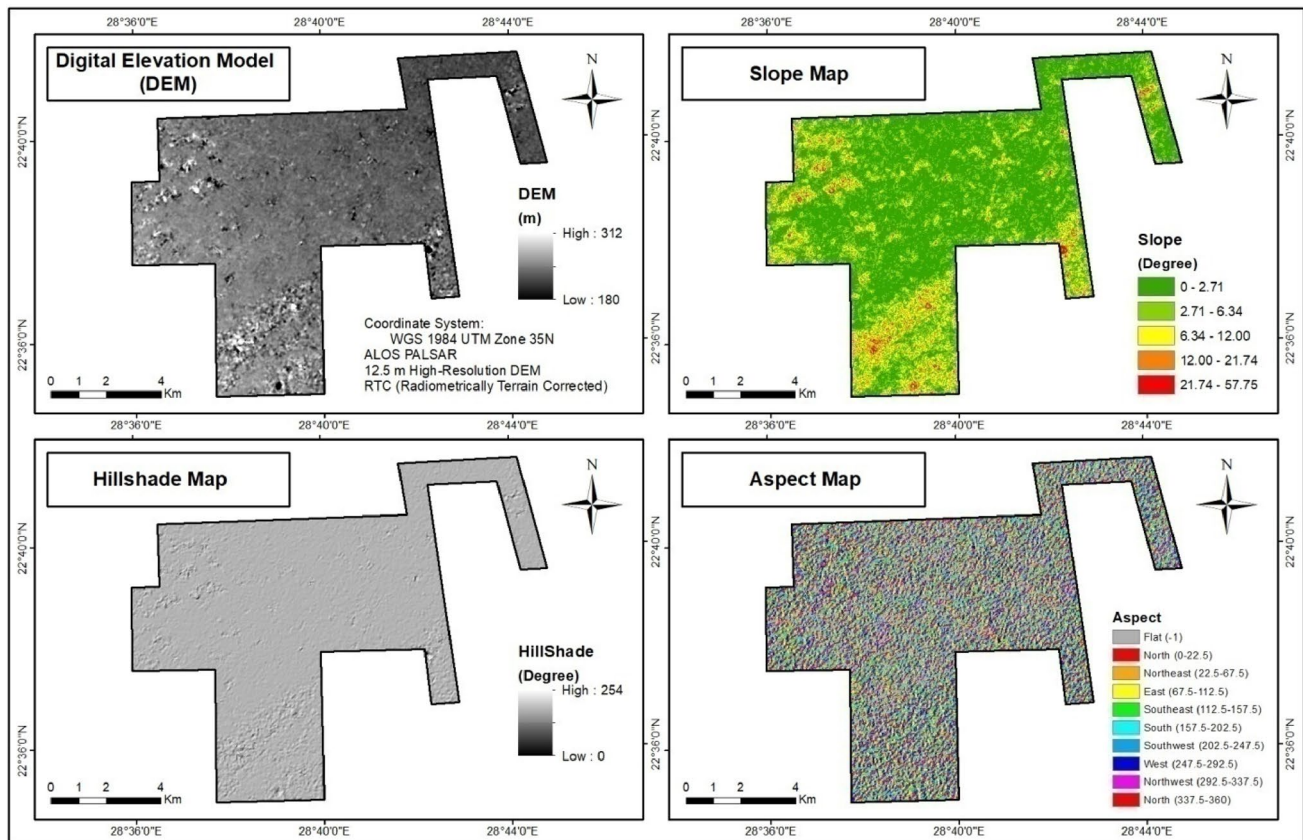


Fig. 5 Digital Elevation Model (DEM), Slope, Hillshade, Aspect maps for the study area

Correlation between well-logging data

To achieve the aim of the study, subsurface data such as geophysical information and hydrogeological data are critical to visualize the aquifer system and to determine the optimal location for drilling new groundwater wells. Well correlation is considered one of the main steps for building up the 3D hydrogeological model.

To visualize the extent of the lithostratigraphic layers within the study area, a total number of 23 cross sections (Fig. 6) have been created. The first 11 subsurface cross sections are constructed in a West–East direction labeled from A1 to A11. The second 12 cross sections have been created in the South–North direction, labeled from B1 to A12. In this article, two cross sections (Fig. 6) will be presented as examples for these subsurface cross sections: (1) cross section A1 in the E–W direction; and (2) cross section B6 in the N–S direction.

Correlation in E–W direction: for example, “cross section A1”

The first cross section A1 (Fig. 7) is constructed to visualize the lateral and vertical extension of the lithofacies along

the E–W direction in the study area. This cross section A1 extends for about 4 km and is encountered with four groundwater wells which are 17 R, 22 R, 27 R and 32 R, respectively, with a distance interval of about 1 km between each well. The dominated stratigraphic units are sandstone aquifers interbedded by thin layers of shales. The gamma-ray log values are high which is attributed to the presence of radioactive materials in shale layers.

In the present study, a re-interpretation of the well-logging data has been carried out to determine the thickness of aquifer layers (sandstone) and aquitard layers (shale). The aquifer thicknesses of the wells 17 R, 22 R, 27 R, and 32 R are 217.8 m, 259.9 m, 256.8 m, and 256.5 m, respectively; while the aquitard thicknesses are 62.2 m, 40.1 m, 41.2 m and 43.5 m, respectively. The static water depth (SWD) for each well is 38.6 m, 34.6 m, 32.2 m, and 33 m, respectively, which indicates that the groundwater flow direction is considered to be in the East direction from the high level to the lowest depth of SWD along this cross section.

For the present study, the optimal well location for drilling groundwater wells is where the aquifer thicknesses increase and aquitard thicknesses decrease, because it allows installing a high length of screen pipes in front of the

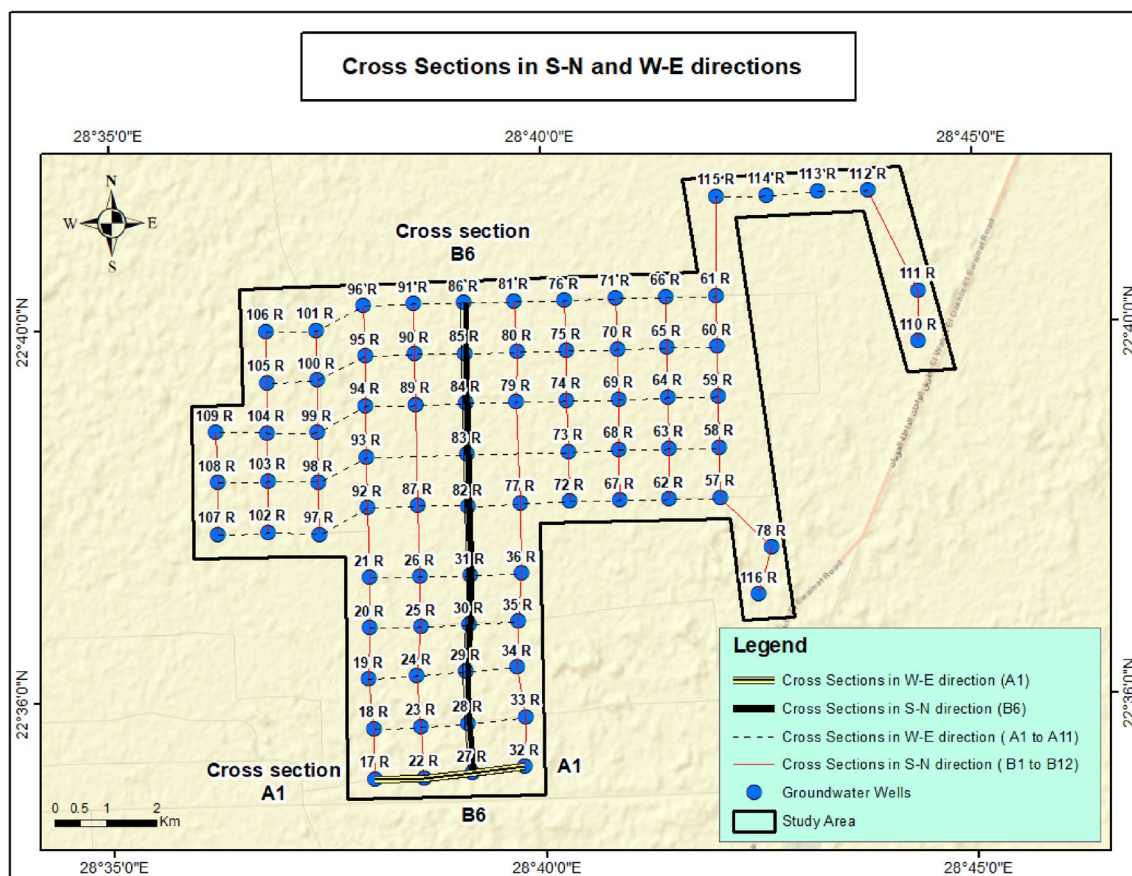


Fig. 6 Location map for the cross sections in S–N and W–E directions within the study area

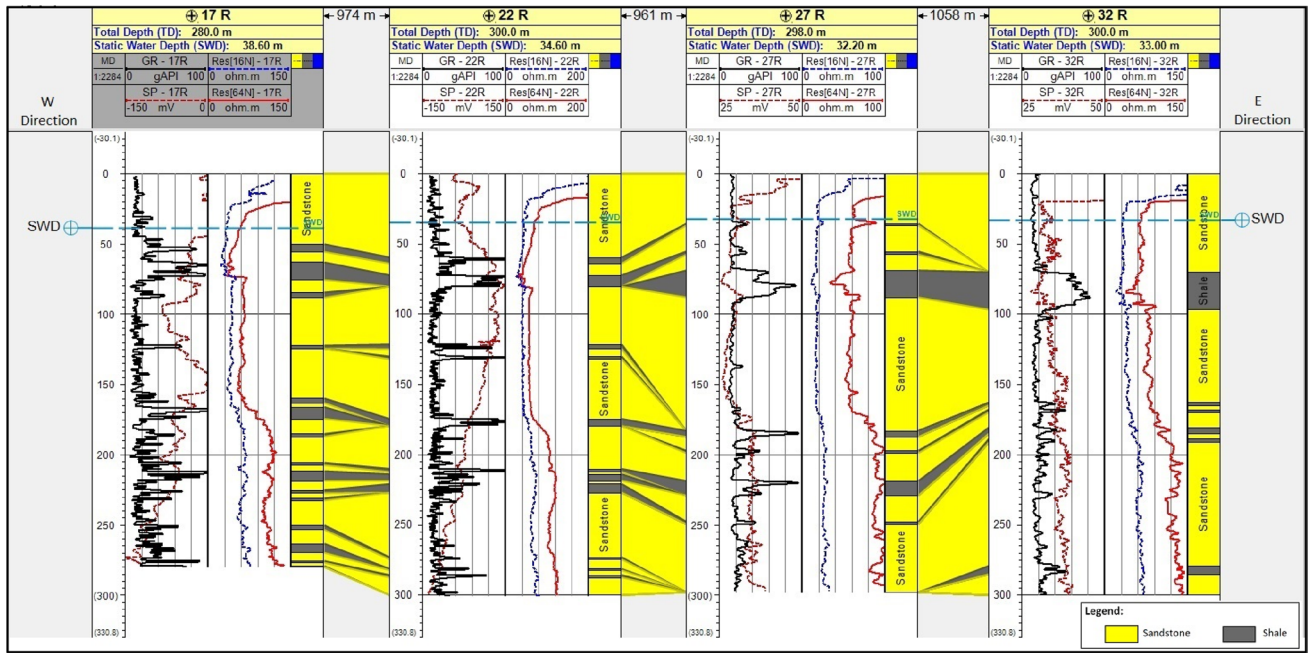


Fig. 7 Subsurface well-logging correlation in W–E direction for the cross section A1

sandstone layers to get the required quantity of the groundwater used for agricultural activities.

Correlation in N–S direction: for example, “cross section B6”

The geologic cross section B6 (Fig. 8) is considered to be one of the 12 cross sections in the N–S direction. This cross section B2 has a distance of about 10 km and is passing through ten groundwater wells which are from south to north; 27 R, 28 R, 29 R, 30 R, 31 R, 82 R, 83 R, 84 R, 85 R and 86 R, respectively, with a distance of about 1 km between wells.

In this cross section B6, the groundwater wells 29 R, 82 R and 84 R (Table 1, Fig. 8) penetrate prominent Precambrian basement rocks in the bottom of these wells which are overlain by the upper Cretaceous Nubian Sandstone aquifer. The presence of basement rocks has been confirmed by the description of borehole cutting samples that were collected during the drilling process.

This cross section B6 (Fig. 8) represents the lateral and vertical distribution of the aquifer lithostratigraphic layers. The total depths have been affected strongly by the appearance of basement rocks, which is considered to be a bad

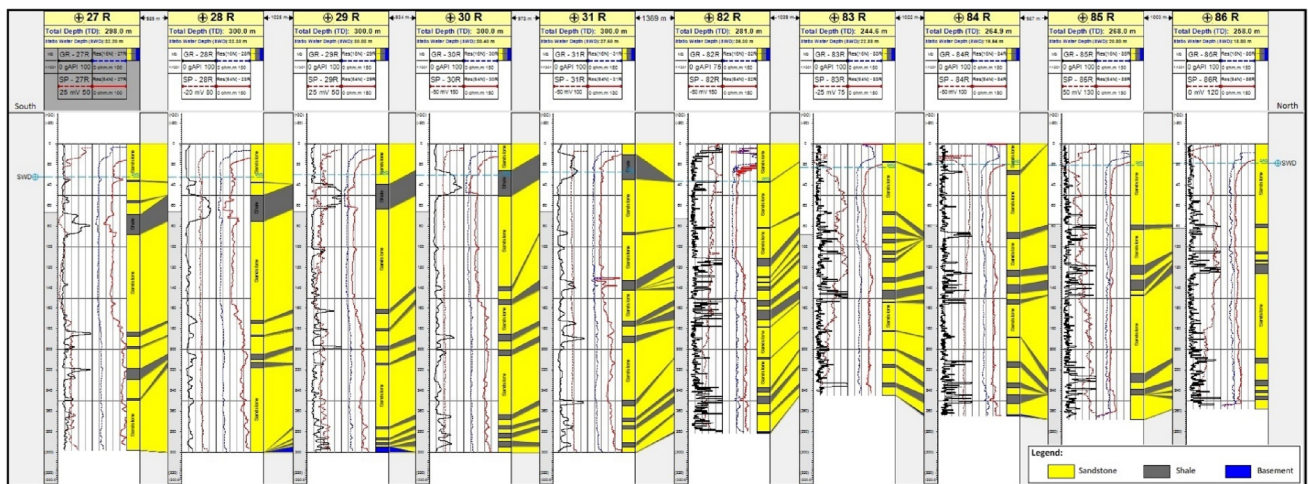


Fig. 8 Subsurface well-logging correlation in S–N direction for the cross section B6

Table 1 Top of basement and thicknesses of each well along the cross section B6 in S–N direction

Well name	Top of basement (m)	Total depth (m)	Aquifer thickness (m)	Aquitard thickness (m)	Static water depth (m)
27 R	–	298	256.8	41.2	32.2
28 R	–	300	258.9	41.1	32.4
29 R	294	295	251.6	43.0	30.0
30 R	–	300	236.2	63.8	30.4
31 R	–	300	237.6	62.4	27.5
82 R	280	281	235.8	44.2	36.3
83 R	–	245	201.5	43.1	22.9
84 R	263	265	214.9	48.1	19.9
85 R	–	268	229.8	38.2	20.8
86 R	–	258	227.1	30.9	18.8

location for drilling groundwater wells due to the absence of aquifer layers beneath these bedrocks.

Aquifer properties and characteristics used for selecting the optimal well site

Static water depth (SWD)

Static water depth (Fig. 9A) ranges between a maximum value of 38.6 m at the well 17 R in the southwest and a minimum value of 13.8 m at the well 114 R in the northeast part of the study area with an average of 24.5 m. The 3D visualization of SWD (Fig. 9A) shows that the groundwater flow direction is considered to be from the northeast towards the deepest points of SWD in the southwest direction.

For the objective of this study, the groundwater flow direction is a very important environmental factor in

choosing the optimal well location for drilling new wells. A well should be placed at a low value of static water depth, so that the contamination from any source moves away from the well and not toward the well. For economic reasons, it is generally better to drill a well uphill rather than downhill. A well with a shallow static water depth will require more pipes and a powerful pump to get the water to the surface, which can be more expensive compared to extracting it from a shallow borehole.

Petrel software enables quick and interactive blending and rendering of multiple subsurface properties. Therefore, a combination of three-dimensional visualization modeling for lithostratigraphic layers and static water depth (Fig. 9B) can be proposed for understanding the groundwater flow direction. In the study area, groundwater flow direction and static water depth are affected by the appearance of basement rocks at the bottom of some groundwater wells.

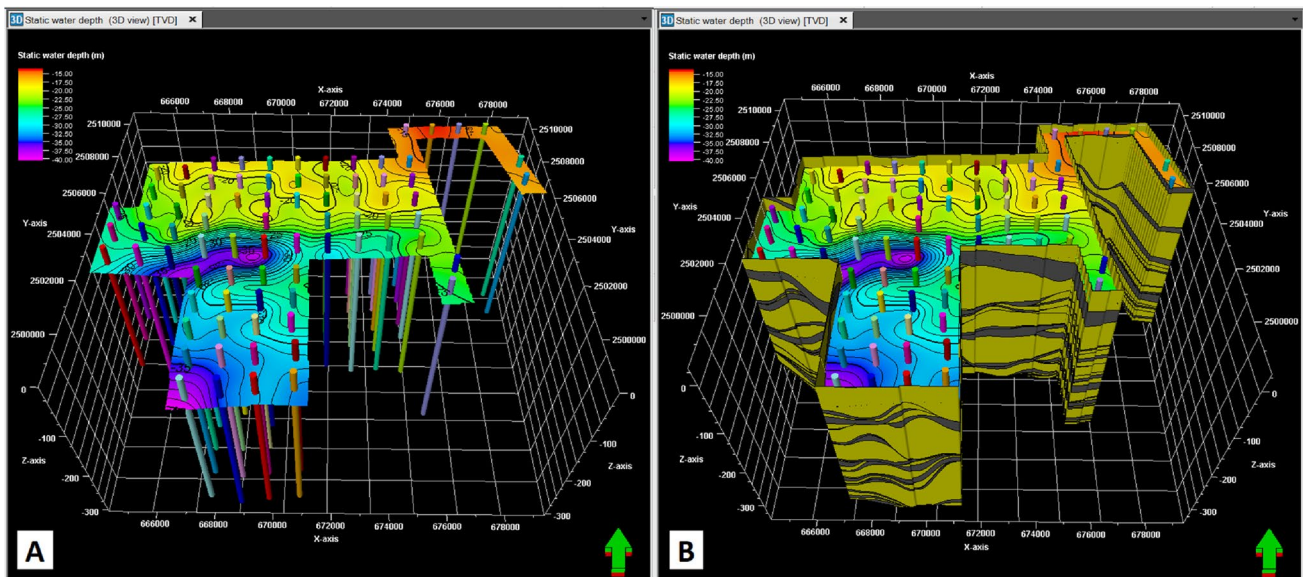


Fig. 9: 3D visualization for: **A** static water depth (m); and **B** static water depth (m) and lithostratigraphic layers in the study area

Aquifer and aquitard thicknesses

Aquifer thickness (Fig. 10A) is one of the major factors that can be used for selecting the optimal site or location for drilling new wells. As the aquifer thickness increases, the suitability of site selection increases because the sandstone layers are capable of serving as a groundwater reservoir and supplying enough water. This is important to satisfy a particular purpose and yield economically significant quantities of water from the groundwater well.

Aquifer thickness in the study area (Fig. 10A) ranges between 269.48 m at well 74 R and 184.00 m at well 101 R in the northwest direction with an average aquifer thickness of 232.26 m. This fluctuation in the aquifer thickness is attributed to the change in the total thickness of the wells which is affected strongly by the appearance of the basement rocks at the bottom of some wells.

On the contrary, as the aquitard thickness (Fig. 10B) decreases, the suitability of site selection increases. The aquitard layers supply the well with fine sediments which may block the slots of the screen pipes over time and break them due to the pressure on these slots. Consequently, increasing of aquitard layers is considered to be a disadvantage in selecting the optimal well site.

The aquitard thickness (Fig. 10B) fluctuates from 78.52 m at well 26 R to 22.59 m at well 81 R with an average aquitard thickness of about 43.90 m throughout the study area. The increase in the aquitard thickness is partially attributed to the decrease in the aquifer thickness and decrease in the total thickness.

Top of the basement and total depth

To identify areas where there is a high probability of successfully drilling groundwater wells, consideration must be given to the extension of basement rocks (Fig. 11A) in the study area. In hydrogeology, drilling groundwater wells in the basement rocks are considered to be a waste of time and money due to the absence of aquifer layers beneath these bedrocks.

In the present study area, basement rocks (Fig. 11A, Table 2) were encountered at the bottom of 31 groundwater wells and were confirmed by cutting samples collected during the drilling process. Therefore, this study strongly recommends not drilling any wells near these sites if the existing wells fail or break down for any reason in the future.

The total depth in the study area (Fig. 11B) varies between 306 m at well 23 R and 227 m at well 106 R with an average total depth of about 277 m. The total penetration depth has been strongly affected by the appearance of basement rocks at the bottom of some wells.

Aquifer loss and well loss coefficients

The behavior of the groundwater well can be summarized by a relationship expressing the drawdown in a pumping well(s) as a function of discharge rate (Q). Therefore, Jacob (1947) first proposed the relationship:

$$S = BQ + CQ^2, \quad (1)$$

where (S) is the drawdown (m), (Q) is the discharge rate (m^3/hr), (B) is the aquifer loss or formation loss coefficient (hr/m^2) and, (C) is the well loss or head loss coefficient

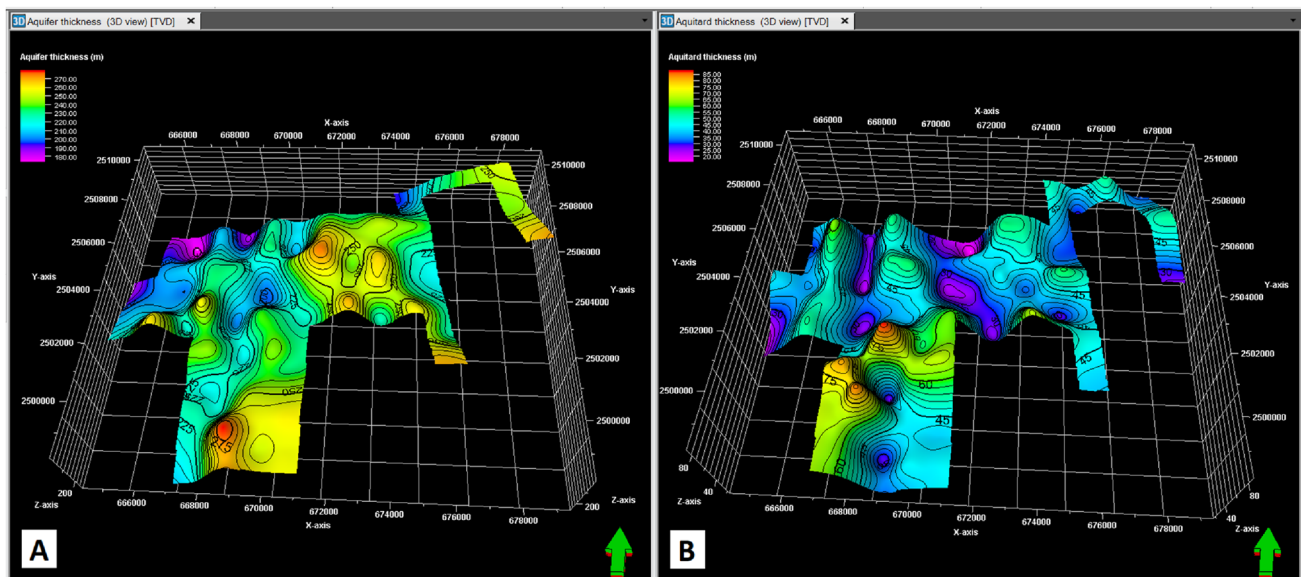


Fig. 10: 3D visualization for: **A** aquifer thickness (m); and **B** aquitard thickness (m) in the study area

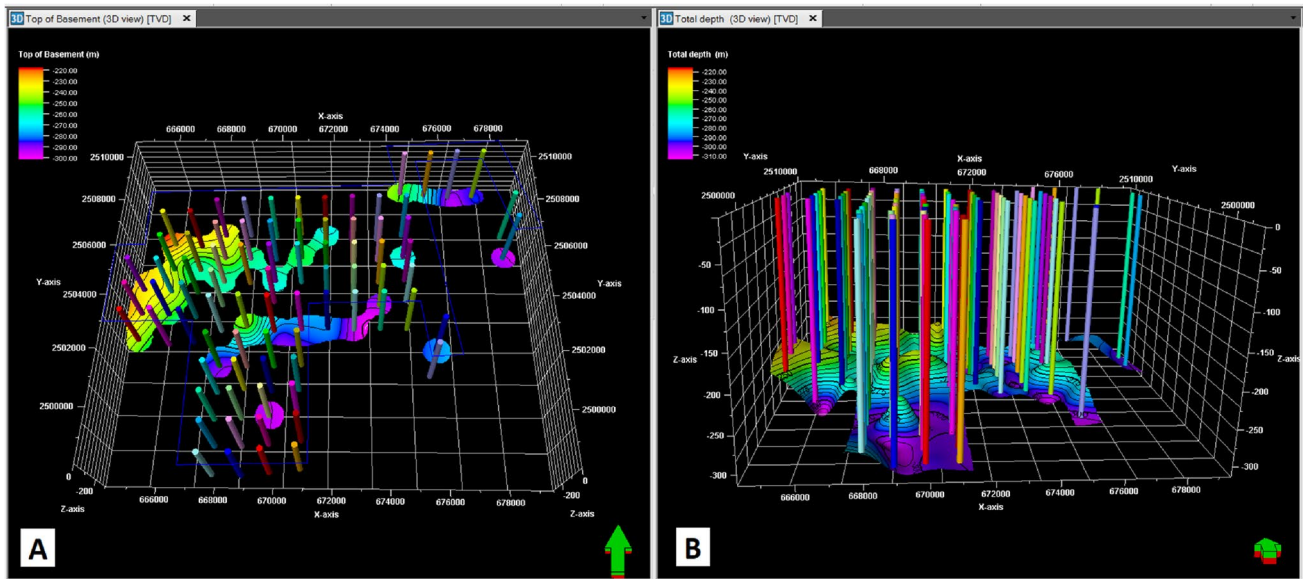


Fig. 11: 3D visualization for: **A** top of basement at the bottom of some wells (m); and **B** total depth of each well (m) in the study area

Table 2 Top of Basement rocks encountered at the bottom of 32 groundwater wells in the study area

Well name	Top of basement (m)	Well name	Top of basement (m)	Well name	Top of basement (m)
21 R	288	84 R	263	106 R	226
29 R	294	87 R	249	107 R	245
60 R	264	90 R	256	108 R	235
63 R	293	94 R	258	109 R	232
67 R	295	95 R	245	110 R	294
72 R	280	96 R	236	112 R	285
76 R	264	100 R	259	113 R	290
77 R	281	101 R	238	114 R	265
78 R	280	103 R	250	115 R	250
80 R	252	104 R	240		
82 R	280	105 R	243		

(hr²/m⁵), (BQ) is the laminar term, and (CQ²) is the turbulent term (Jacob 1947).

Aquifer loss coefficient (B) (Fig. 12A) has been determined for the 79 wells in the study area and it ranges from a maximum value of 0.19 hr/m² at well 102 R and a minimum value of 0.003 hr/m² at well 63 R with an average value of 0.069 hr/m². Increasing the aquifer loss coefficient is attributed to the effect of drilling mud. This mud plugs the aquifer during the drilling process and leads to increasing the aquifer loss coefficient because this drilling mud reduces the permeability near the borehole well (Poehls and Smith 2009).

Well loss coefficient (C) (Fig. 12B) varies between a maximum value of 0.0005 hr²/m⁵ at well 96 R and a minimum value of 0.000013 hr²/m⁵ at well 111 R with an average value of 0.000090 hr²/m⁵. The increase in well loss coefficient (C) is caused mainly by the well design and the degree of well development rather than the aquifer properties and shale layers.

Both aquifer loss coefficient (B) and well loss coefficient (C) strongly affect the well efficiency of the groundwater well. The well efficiency of the pumped well is calculated as the ratio of laminar head loss (aquifer loss) to total head loss (Mogg 1969; Todd 1980).

Well efficiency and total dissolved solids (TDS)

Well efficiency can be determined by analyzing the step-drawdown tests which are performed inside the borehole without the use of monitoring well(s) (Kruseman and de Ridder 1990). Well efficiency can be calculated from the following equation:

$$\text{Wellefficiency}(\%) = \frac{BQ}{(BQ + CQ^2)} \times 100, \tag{2}$$

where (BQ) is the aquifer loss or laminar head loss (m), (CQ²) is the well loss or turbulent head loss (m), (BQ+CQ²) is the Total head loss (m), and (Q) is the discharge rate (m³/hr.).

In the present study, the well efficiency (Fig. 13A) has been determined for 79 groundwater wells in the study area by applying the above Eq. (2). The safe yield for most groundwater wells in the study area occurs at a discharge

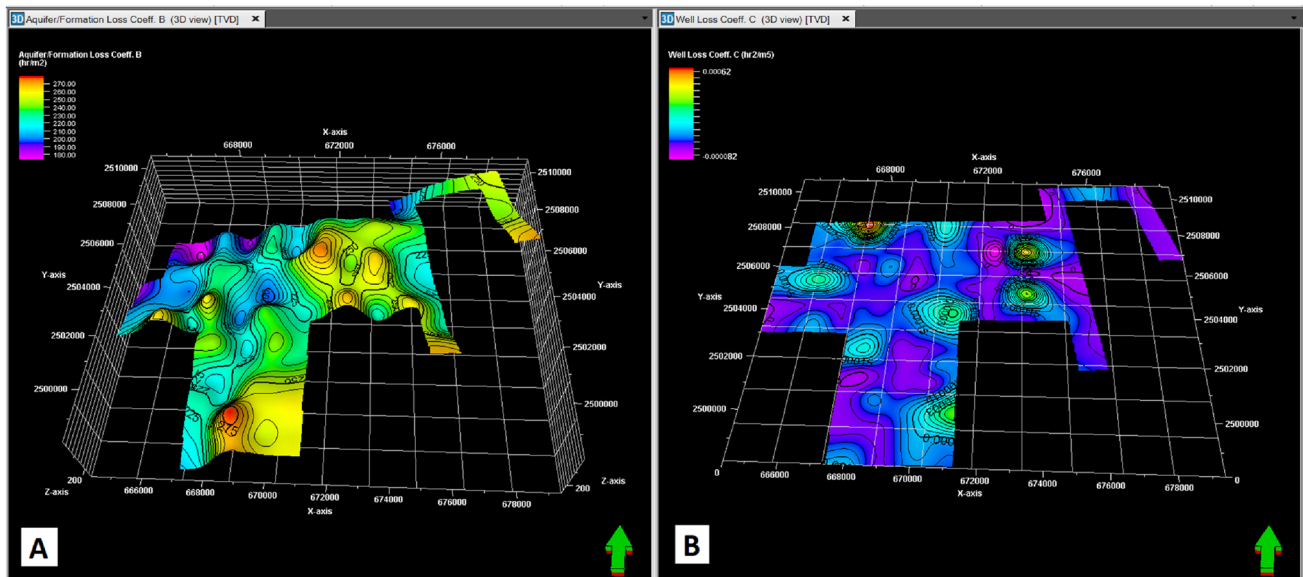


Fig. 12: 3D visualization for: **A** aquifer loss coefficient; and **B** well loss coefficient in the study area

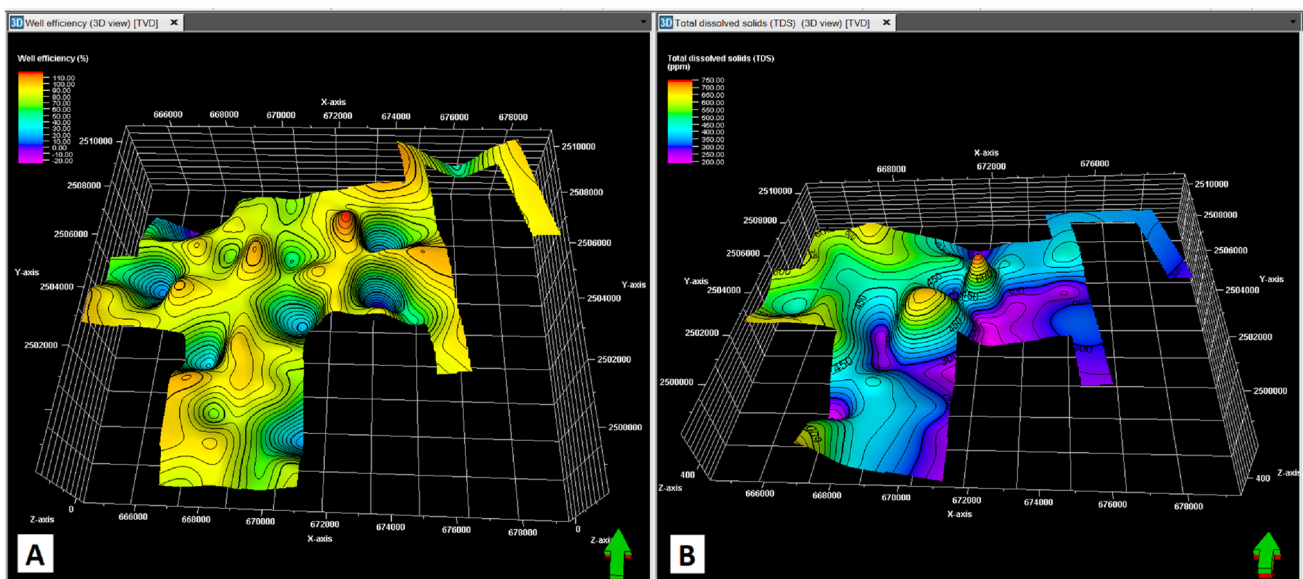


Fig. 13: 3D visualization for: **A** well efficiency; and **B** total dissolved solids (TDS) in the study area

rate Q of 250 m³/hr. (RIGW 2008). The well efficiency reached a maximum value of 95.91% at well 66 R, while the minimum values of the well efficiency recorded 3.85%, 8.76%, 9.91%, 16.67%, 20.56%, 25.74%, 29.91%, 38.27%, at wells 63 R, 96 R, 65 R, 104 R, 101 R, 77 R, 33 R, 21 R, respectively. These very low values of well efficiency are attributed to the effects of insufficient well development or inappropriate well design and construction. Consequently, this can cause failure or break down of these wells shortly after construction. Therefore, it is highly recommended to

perform the air development and pump development stages to increase the well efficiency of these wells (Poehls and Smith 2009).

In the study area, total dissolved solids (TDS) (Fig. 13B) range between 690 mg/l at well 74 R and 230 mg/l at well 67 R. Therefore, according to (Chebotarev 1955) classification for salinity, the groundwater in the study area belongs to the freshwater type which ranges between 0 and 1000 mg/liter.

Building up 3D hydrogeological modeling and visualization of aquifer system based on borehole data

3D visualization of aquifer system: (view from North, South, East and West directions)

The establishment of three-dimensional hydrogeological modeling for the aquifer system in the study area will play a pivotal role in groundwater development and management. This 3D hydrogeological modeling and visualization of the aquifer system can provide a better understanding of the aquifer system and can be used as a decision-aiding tool for selecting the optimal site or location for drilling new groundwater wells in the future. The geophysical and hydrogeological data collection enabled a good spatial distribution of the geological information.

For the present study, Petrel software allows the viewer to visualize the 3D model from different directions (North, South, East, and West) (Fig. 14). Visualizing objects in 3D view allows the users and decision-makers to observe details that would have been lost by looking at them in 2D view. Therefore, the decision maker can easily understand and view the lateral and vertical distribution of the lithostratigraphic layers (sandstone, shale, and basement layers). Hence the 3D model can be used as a tool to determine and select the optimal location for drilling new wells by determining the areas of high aquifer thicknesses and low aquitard thicknesses and by putting plans for the design of

the wells (screen pipes and blank pipes) according to the distribution of the lithostratigraphic layers.

Grids in J-directions

For visualization of the 3D model, I- and J-intersections are two intersections perpendicular to each other along the grid lines in the 3D hydrogeological model. Petrel enables the use of the so-called “Intersection player” to step and navigate through the various intersections in the 3D model (Petrel 2017).

In the present study, 4 grids in J-directions (Fig. 15) have been created as an example to visualize the 3D model and the lithostratigraphic layers of the aquifer system in specific sites inside the area of study. Two grids in J-directions are located in the north part of the study area and labeled 1A and 2A. The other 2 grids are labeled 3A and 4A and located in the south part of the study area.

Satellite imagery of Landsat L8 OLI-TIRS has been used as a surface layer for visualization of the study area with a band combination of natural color 4, 3, 2 (RGB) and transparency of 70%. The surface satellite imagery shows circles that represent the cultivated areas as appear on the left side (Fig. 15). These agricultural areas appear like circles due to the use of the “Center pivot irrigation” system. While the resulting 4 cross sections (4 grids in J-intersections) represent the subsurface vertical and lateral distribution of the lithostratigraphic layers (sandstone, shale, and basement layers) in the study area.

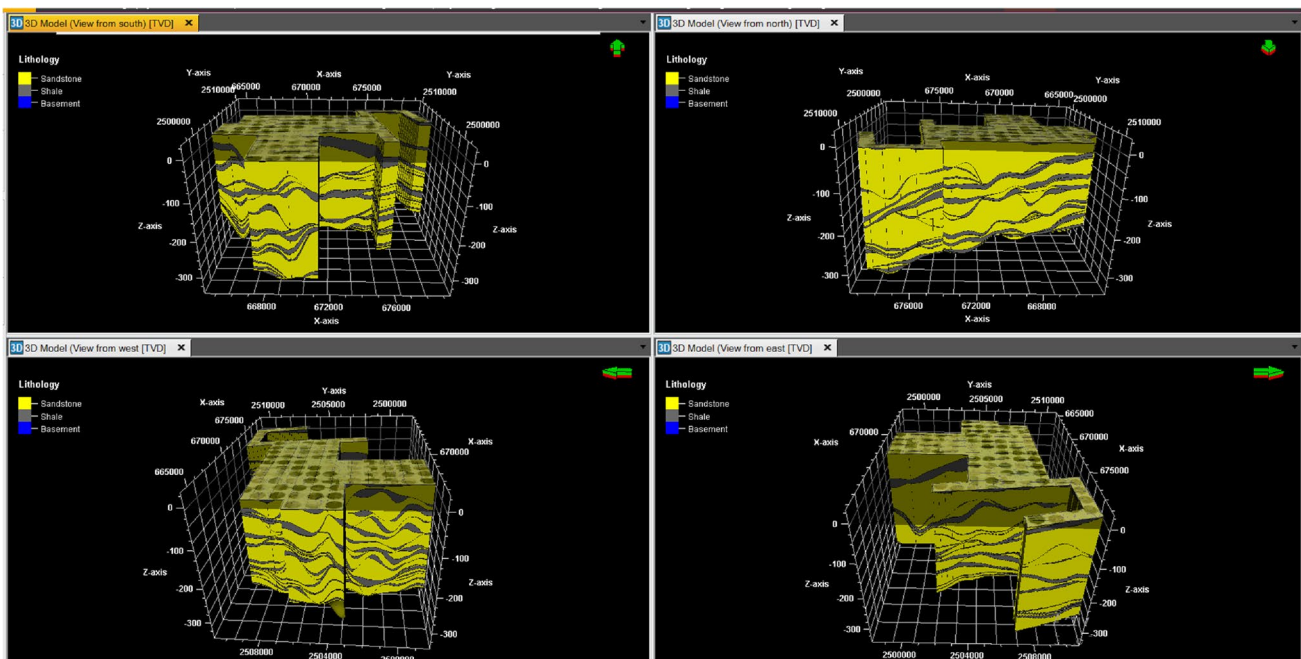


Fig. 14 Three-dimensional visualization model of the aquifer system (View from North, South, East and West directions)

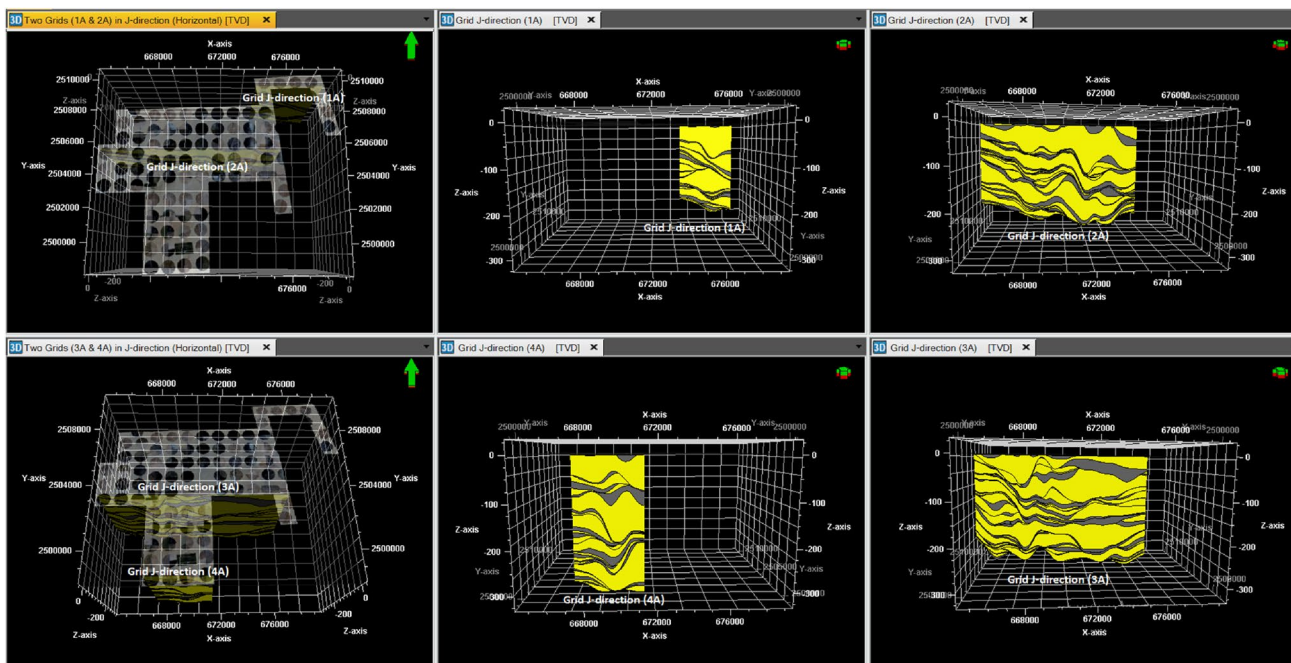


Fig. 15 Four grids (1A, 2A, 3A, 4A) in J-directions for visualization of aquifer system with satellite image as a surface

Grids in I-directions

Petrel software enables using the spin animation tool for rotation of the 3D model as appears on the left side (Fig. 16). Therefore, another 4 grids in I-directions

(labeled 1B, 2B, 3B, and 4B) have been created perpendicular to the previous J-direction to visualize the change in the lithofacies in another direction throughout the study area. These I- and J-direction intersections are stored in the 3D Model pane in the intersections folder and the

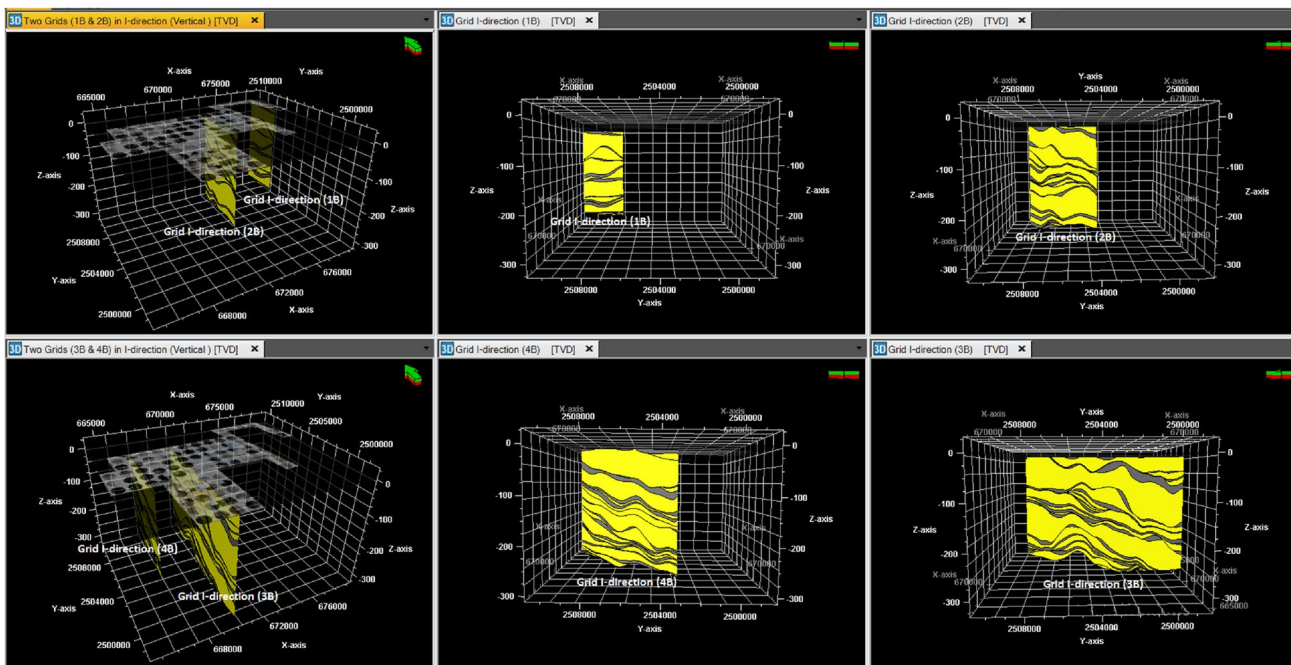


Fig. 16 Four grids (1B, 2B, 3B, 4B) in I-directions for visualization of aquifer system with satellite image as a surface

intersection player tool can be used to visualize multiple cross sections at any location in the area under investigation. Animation and playing the intersection player tool through the 3D model using the general intersection planes is a very efficient method for increasing the understanding and visualization of the 3D model.

The cross sections on the right side (Fig. 16) show that the aquifer system can be divided into small sub-aquifers separated by aquitard layers of shale. Moreover, the modeled lithostratigraphic units can be combined with the previously discussed aquifer properties to determine the optimal site or location for drilling new wells based on several parameters and characteristics of the aquifer system which can achieve the main objective of this study.

Distribution of lithofacies in the study area

The 3D hydrogeological model can quickly display the three-dimensional shape for the lateral and vertical distribution of the lithofacies (sandstone, shale, and basement) in the study area (Fig. 17). Improving the 3D visibility of the geological body can provide a basis for the design of new boreholes. The establishment of 3D modeling greatly promotes the visual development and management of aquifer systems. It can also provide a reasonable prediction of the optimal site or location for drilling new wells by choosing the areas of high aquifer thicknesses of sandstone layers and low shale layers. For selecting an optimal location for drilling new wells, it's very important to avoid drilling new wells where basement rocks have been encountered at

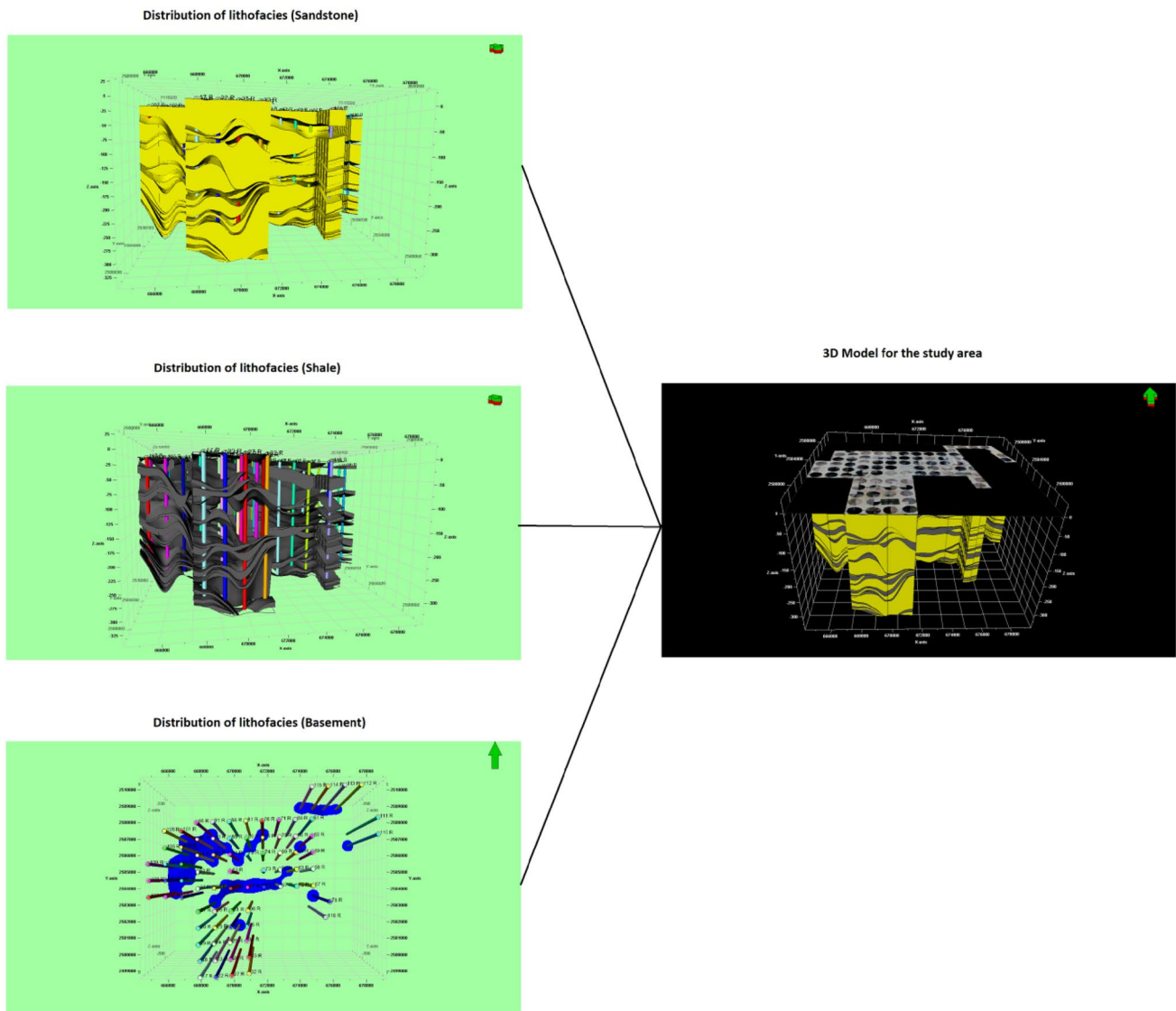


Fig. 17 Distribution of lithofacies (e.g., sandstone, shale and basement) in the study area

shallow depths due to the absence of aquifer layers beneath these bedrocks. Therefore, this 3D hydrogeological model can provide a platform for not only selecting the optimal site for drilling new wells, but also determining the well design.

Conclusions

The combination of the 3D model and the visualization of the lithostratigraphic layers with the aquifer properties can help to make a decision to understand the aquifer system in the study area and to identify the optimal well sites and locations for drilling new wells. These aquifer properties and characteristics include: static water depth; aquifer and aquitard thicknesses; top of the basement and total depth; aquifer loss and well loss coefficients; well efficiency; and total dissolved solids (TDS). Based on the results of the present study, it is highly recommended not to drill any groundwater wells near the 31 wells (Table 2) even if these wells break down or fail for any reason at any time in the future. Because the basement rocks encountered at the bottom of these wells as demonstrated by mapping the extension of the basement rocks in the area of study (Fig. 11A). The 3D hydrogeological model (Fig. 17) can help the decision-makers to visualize the lateral and vertical distribution of the lithofacies and can help put plans for the well design. These plans include determining the length and the position of the pipes inside the borehole well because screen pipes should be placed in front of sandstone layers to get a high quantity of water, while blank pipes should be installed in front of shale layers to prevent fine sediments and to obtain clean water from the borehole.

Three factors and suggestions for improving this 3D hydrogeological model can be summarized as follows: (1) establishing a multi-source 3D model using various geophysical data such as seismic, geoelectric, and electromagnetic data to determine the deep structure; (2) creating dynamic 4D modeling by scheduling measurements for the static water depth inside the wells to determine the fluctuation of the water level over the time; and (3) building a massive 3D data storage using all the 1600 groundwater wells that exist in the regional area of El-Oweinat not only the 79 wells that we used in the present study.

Acknowledgements The first author is funded by scholarship No. EGY 6827/19 under the joint executive program between the Ministry of Higher Education of the Arab Republic of Egypt and the Ministry of Science and Higher Education of the Russian Federation. The authors are grateful to the Department of Geophysics, Novosibirsk State University for its Laboratory that is equipped with the latest version of Petrel software and for allowing the first author to attend several online courses with Schlumberger Company to learn and practice on Petrel software.

Declarations

Conflict of interest The authors confirm that there are no known conflicts of interest associated with this publication and there has been no significant financial support for this work that could have appeared to influence the work reported in this paper.

References

- Abdelhaleem F, Helal E (2015) Impacts of Grand Ethiopian Renaissance Dam on different water usages in upper Egypt. *Br J Appl Sci Technol* 8:461–483. <https://doi.org/10.9734/bjast/2015/17252>
- Al-Temamy A, Barseem M (2010) Structural impact on the groundwater occurrence in Nubia sandstone aquifer using geomagnetic and geoelectrical techniques, Northwest Bir Tarfawi, East El Oweinat area, Western Desert. *Egypt Geophys Soc EGS J* 8:47–63
- Anomohanran O, Oseme JI, Iserhien-Emekeme RE, Ofomola MO (2021) Determination of groundwater potential and aquifer hydraulic characteristics in Agbor, Nigeria using geo-electric, geophysical well logging and pumping test techniques. *Model Earth Syst Environ* 7:1639–1649. <https://doi.org/10.1007/s40808-020-00888-6>
- Araffa SAS, Bedair S (2021) Application of land magnetic and geoelectrical techniques for delineating groundwater aquifer: case study in East Oweinat, Western Desert Egypt. *Nat Resour Res* 30:4219–4233. <https://doi.org/10.1007/s11053-021-09937-y>
- Artimo A, Mäkinen J, Berg RC et al (2003) Three-dimensional geologic modeling and visualization of the Virtaankangas aquifer, southwestern Finland. *Hydrogeol J* 11:378–386. <https://doi.org/10.1007/s10040-003-0256-6>
- Best DM, Lewis RR (2010) GWVis: a tool for comparative groundwater data visualization. *Comput Geosci* 36:1436–1442. <https://doi.org/10.1016/j.cageo.2010.04.006>
- Chebotarev II (1955) Metamorphism of natural waters in the crust of weathering—1. *Geochim Cosmochim Acta* 8:22–48. [https://doi.org/10.1016/0016-7037\(55\)90015-6](https://doi.org/10.1016/0016-7037(55)90015-6)
- CONOCO (1987) Stratigraphic Lexicon and Explanatory Notes to the Geologic map of Egypt 1:500,000. In: Hermina, Maurice, Eberhard, Franz K. List (eds)
- Cox ME, James A, Hawke A, Raiber M (2013) Groundwater Visualisation System (GVS): a software framework for integrated display and interrogation of conceptual hydrogeological models, data and time-series animation. *J Hydrol (amst)* 491:56–72. <https://doi.org/10.1016/j.jhydrol.2013.03.023>
- Datta A, Gaikwad H, Kadam A, Umrikar BN (2020) Evaluation of groundwater prolific zones in the unconfined basaltic aquifers of Western India using geospatial modeling and MIF technique. *Model Earth Syst Environ* 6:1807–1821. <https://doi.org/10.1007/s40808-020-00791-0>
- Ebraheem A, Riad S, Wycisk P, Seif El-Nasr A (2002) Simulation of impact of present and future groundwater extraction from the non-replenished Nubian Sandstone Aquifer in southwest Egypt. *Environ Geol* 43:188–196. <https://doi.org/10.1007/s00254-002-0643-7>
- Ebraheem AM, Garamoon HK, Riad S et al (2003) Numerical modeling of groundwater resource management options in the East Oweinat area, SW Egypt. *Environ Geol* 44:433–447. <https://doi.org/10.1007/s00254-003-0778-1>
- Fajana AO (2020) Integrated geophysical investigation of aquifer and its groundwater potential in phases 1 and 2, Federal University Oye-Ekiti, south-western basement complex of Nigeria. *Model Earth Syst Environ* 6:1707–1725. <https://doi.org/10.1007/s40808-020-00785-y>

- Gill B (2009) Improving knowledge and understanding of groundwater resources using 3D visualisation and quantification tools milestone 4 report: literature review and national round-up/Bruce Gill. Dept. of Primary Industries, Tatura, Vic
- GPC (1984) Hydro-agricultural study project, East Oweinat region, western Desert, Egypt
- Ibrahim SMM (2019) Effects of groundwater over-pumping on the sustainability of the Nubian Sandstone Aquifer in East-Oweinat Area Egypt. *NRIAG J Astron Geophys* 8:117–130. <https://doi.org/10.1080/20909977.2019.1639110>
- Iserhien-Emekeme RE, Ofomola MO, Ohwohere-Asuma O et al (2021) Modelling aquifer parameters using surficial geophysical techniques: a case study of Ovwian, Southern Nigeria. *Model Earth Syst Environ* 7:2297–2312. <https://doi.org/10.1007/s40808-020-01030-2>
- Jacob CE (1947) Drawdown test to determine effective radius of artesian well. *Trans Am Soc Civ Eng* 112:1047–1070
- Karami S, Jalali M, Karami A et al (2022) Evaluating and modeling the groundwater in Hamedan plain aquifer, Iran, using the linear geostatistical estimation, sequential Gaussian simulation, and turning band simulation approaches. *Model Earth Syst Environ* 8:3555–3576. <https://doi.org/10.1007/s40808-021-01295-1>
- Kazakis N, Chalikakis K, Mazzilli N et al (2018) Management and research strategies of karst aquifers in Greece: literature overview and exemplification based on hydrodynamic modelling and vulnerability assessment of a strategic karst aquifer. *Sci Total Environ* 643:592–609. <https://doi.org/10.1016/j.scitotenv.2018.06.184>
- Klitzsch E (1979) Major subdivisions and depositional environments of Nubia strata, Southwestern, Egypt. *Bull. Amer. Assoc. Petroleum Geologists*, Tulsa
- Klitzsch E (1984) Northwestern Sudan and bordering areas: geological development since Cambrian Time. Results of the Special Research Project Arid Areas, Berlin
- Kruseman GP, de Ridder NA (1990) Analysis and evaluation of pumping test data, 2nd ed. International Institute for Land Reclamation and Improvement, Wageningen, The Netherlands
- Li N, Song X, Xiao K et al (2018) Part II: A demonstration of integrating multiple-scale 3D modelling into GIS-based prospectivity analysis: a case study of the Huayuan-Malichang district, China. *Ore Geol Rev* 95:292–305. <https://doi.org/10.1016/j.oregeorev.2018.02.034>
- Li J, Wang W, Cheng D et al (2021) Hydrogeological structure modeling based on an integrated approach using multi-source data. *J Hydrol (amst)* 600:126435. <https://doi.org/10.1016/j.jhydrol.2021.126435>
- Márquez Molina JJ, Lemeillet AF, Sainato CM (2021) Hydrogeological conceptual model of an irrigated agricultural area, Buenos Aires Province Argentina. *Groundw Sustain Dev* 12:100486. <https://doi.org/10.1016/j.gsd.2020.100486>
- Masoud MH, Schneider M, el Osta MM (2013) Recharge flux to the Nubian Sandstone aquifer and its impact on the present development in southwest Egypt. *J Afr Earth Sci* 85:115–124. <https://doi.org/10.1016/j.jafrearsci.2013.03.009>
- Mogg JL (1969) Step-drawdown test needs critical review. *Groundwater* 7:28–34. <https://doi.org/10.1111/j.1745-6584.1969.tb01265.x>
- Nour S (1996) Groundwater potential for irrigation in the East Oweinat area, Western Desert Egypt. *Environ Geol* 27:143–154. <https://doi.org/10.1007/BF00770426>
- Oguama BE, Ibuot JC, Obiora DN, Aka MU (2019) Geophysical investigation of groundwater potential, aquifer parameters, and vulnerability: a case study of Enugu State College of Education (Technical). *Model Earth Syst Environ* 5:1123–1133. <https://doi.org/10.1007/s40808-019-00595-x>
- Petrel (2017) Petrel Software Manual, Schlumberger Information Solutions
- Poehls DJ, Smith GJ (2009) *Encyclopedic dictionary of hydrogeology*, 1st edn. Academic Press/Elsevier, Amsterdam
- Qiao Y-K, Peng F-L, Wu X-L, Luan Y-P (2022) Visualization and spatial analysis of socio-environmental externalities of urban underground space use: Part 2 negative externalities. *Tunnell Undergr Space Technol* 121:104326. <https://doi.org/10.1016/j.tust.2021.104326>
- Rane N, Jayaraj GK (2021) Stratigraphic modeling and hydraulic characterization of a typical basaltic aquifer system in the Kadva river basin, Nashik, India. *Model Earth Syst Environ* 7:293–306. <https://doi.org/10.1007/s40808-020-01008-0>
- RIGW (2008) Research Institute for Ground Water. Internal Report about the potentiality of groundwater in East El-Oweinat area
- Robins NS, Rutter HK, Dumbleton S, Peach DW (2005) The role of 3D visualisation as an analytical tool preparatory to numerical modelling. *J Hydrol (amst)* 301:287–295. <https://doi.org/10.1016/j.jhydrol.2004.05.004>
- Ross M, Parent M, Lefebvre R (2005) 3D geologic framework models for regional hydrogeology and land-use management: a case study from a Quaternary basin of southwestern Quebec, Canada. *Hydrogeol J* 13:690–707. <https://doi.org/10.1007/s10040-004-0365-x>
- Samadi J (2022) Modelling hydrogeological parameters to assess groundwater pollution and vulnerability in Kashan aquifer: novel calibration-validation of multivariate statistical methods and human health risk considerations. *Environ Res* 211:113028. <https://doi.org/10.1016/j.envres.2022.113028>
- Tian Y, Zheng Y, Zheng C (2016) Development of a visualization tool for integrated surface water–groundwater modeling. *Comput Geosci* 86:1–14. <https://doi.org/10.1016/j.cageo.2015.09.019>
- Todd DK (1980) *Groundwater hydrology*, 2nd edition. Geol Mag 118:535. <https://doi.org/10.1017/S0016756800032477>
- Zhu L, Zhang C, Li M et al (2012) Building 3D solid models of sedimentary stratigraphic systems from borehole data: an automatic method and case studies. *Eng Geol* 127:1–13. <https://doi.org/10.1016/j.enggeo.2011.12.001>

Publisher's Note Springer Nature remains neutral with regard to jurisdictional claims in published maps and institutional affiliations.

Springer Nature or its licensor holds exclusive rights to this article under a publishing agreement with the author(s) or other rightsholder(s); author self-archiving of the accepted manuscript version of this article is solely governed by the terms of such publishing agreement and applicable law.